Screening the Coulomb interaction and thermalization of Anderson insulators

Z. Ovadyahu
Racah Institute of Physics, The Hebrew University, Jerusalem 91904, Israel

(Received 17 March 2019; revised manuscript received 20 May 2019; published 31 May 2019)

Long-range interactions are relevant for a wide range of phenomena in physics where they often present a challenge to theory. In condensed matter, the interplay of Coulomb interaction and disorder remains largely an unsolved problem. In two-dimensional films the long-range part of the Coulomb interaction may be screened by a nearby metallic overlay. This technique is employed in this work to present experimental evidence of its effectiveness in limiting the spatial range of the Coulomb interaction. We use this approach to study the effects of the long-range Coulomb interaction on the out-of-equilibrium dynamics of electron glasses using amorphous indium oxide films. The results demonstrate that electronic relaxation times, extending over thousands of seconds, do not hinge on the long-range Coulomb interaction or on the presence of a real gap in the density of states. Rather, they emphasize the dominant role played by disorder in controlling the slow thermalization processes of Anderson insulators taken far from equilibrium.

DOI: 10.1103/PhysRevB.99.184201

I. INTRODUCTION

The interplay between disorder and Coulomb interaction has been a challenging problem in condensed-matter physics. Effects associated with disorder while neglecting interaction may still be a difficult problem to solve. Such theories, however, are rarely applicable for experiments as disorder and interactions appear to be connected; increasing one usually increases the other. Few comprehensive studies treating disorder and interactions have been carried out, and those that have been done are usually for cases when both disorder and interactions are fairly weak or when the spatial range of the interaction is limited. In the strong-disorder regime, however, neglecting the long-range part of the interaction is difficult to justify, thus further compounding a difficult problem. This is true in particular for the Anderson localization case where the question of Coulomb interaction that originated decades ago [1,2] is still unsolved despite extensive efforts. Some progress has been made on this many-body problem for short-range interaction [3–5], but effects of the long-range component are yet largely unresolved.

An intriguing result of the disorder-interaction competition is the appearance of a nonergodic phase exhibiting glassy features. These involve slow conductance relaxations of Anderson insulators taken far from the equilibrium and a variety of memory effects [6,7]. Relaxation times that extend over thousands of seconds are observable at temperatures where the hopping length, which is the effective screening length in the insulating regime, is of the order of 20 nm.

Theoretical models that qualitatively account for these effects are based on the opening up of a soft gap [8–15] in the system density of states (DOS). This so-called Coulomb gap [16] is reflected in the conductance G versus gate voltage V_g as a cusplike minimum centered at the point where the system was allowed to relax (the "memory dip") [7]. To be observable in $G(V_g)$ scans, $\partial V_g/\partial t$ must be fast enough relative to the relaxation rate of the electronic system [17]. For technical reasons this condition limits the choice of systems to Anderson insulators with relatively high carrier concentration N where both disorder and interactions are strong [17]. The importance of strong disorder and interaction is attested to by the seven different systems that exhibit these nonequilibrium effects, all sharing the feature of high carrier concentration $N \gtrsim 10^{19}\,\mathrm{cm}^{-3}$. It is yet not clear, however, what role is played by the long-range Coulomb interaction in these phenomena.

In this work we attempt to find answers to this and related questions by using a metallic ground plane in proximity to the sample to modify the long-range Coulomb interaction in a controlled way. Using samples configured for field-effect measurements and furnished with a nearby screening plane yields results consistent with the anticipated [18] outcome for a modified Coulomb gap. The dynamics of these systems, on the other hand, does not show a significant difference from the reference samples. It seems therefore that, in addition to strong enough quenched disorder, short- and medium-range interactions may be sufficient to account for the long relaxation times observed in the experiments. In particular, the results demonstrate that relaxation times extending over hours are sustainable in interacting Anderson insulators even while having a finite density-of-states at the chemical potential.

To optimize the effect of screening by a nearby metal, the system chosen for the study had rather low carrier concentration. This also resulted in systems with short relaxation times. We took advantage of the latter to systematically study the deviation from the logarithmic relaxation law to elucidate the relative importance of disorder and interaction to the slow dynamics of the glassy phase.

II. EXPERIMENT

Sample preparation and measurement techniques

Samples used in this study were 200-Å-thick films of In_xO. These were made by e-gun evaporation of 99.999%

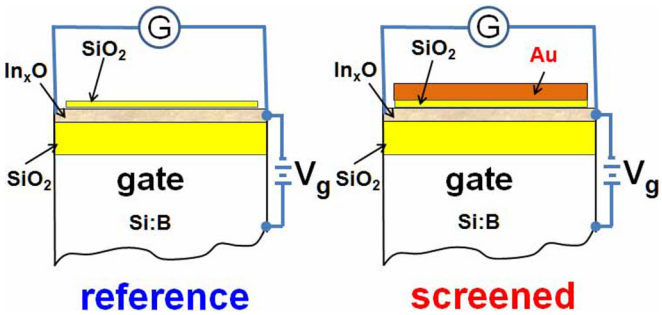

FIG. 1. Schematic description of the reference and screened samples configured for field-effect measurements.

pure In_2O_3 onto room-temperature Si wafers in a partial pressure of 1.5×10^{-4} mbar of O_2 and a rate of 0.5 ± 0.1 Å/s. The Si wafers (boron doped with bulk resistivity $\rho \leqslant 2 \times 10^{-3}\,\Omega\,\mathrm{cm}$) were employed as the gate electrode in the field-effect and gate-excitation experiments. The samples were deposited on a SiO_2 layer (2 μm thick) that was thermally grown on these wafers and acted as the spacer between the sample and the conducting Si:B substrate.

The as-deposited films had sheet resistance $R_\square > G\Omega$ at room temperature. They were then thermally treated. This was done by stages; the samples were held at a constant temperature starting from ≈340 K for 20–30 h; then the temperature was raised by 5–10 K for the next stage. This was repeated until the desired $R_\square$ was attained (see [19] for fuller details of the thermal annealing and structure analysis). This process yielded samples with $R_\square = 18$–45 kΩ that at $T \approx 4$ K spanned the range of 100 kΩ to 40 MΩ. The carrier concentration N of these samples, measured by the Hall effect at room temperature, was in the range $N = 8.7 \times 10^{18}$ to $2 \times 10^{19}\,\mathrm{cm}^{-3}$. The main focus in this work is a study of the effects produced by screening the long-range part of the Coulomb interaction on the nonequilibrium transport of Anderson insulators. The experimental methodology we employ is comparing simultaneously deposited samples, placing a metallic plane in close proximity to just one of them. Figure 1 illustrates the geometry of the pair of samples, labeled "screened" and "reference," each configured for field-effect measurements.

The distance between the screened sample and the screening layer (an ≈200 Å gold film) is determined by the thickness d of the SiO_2 layer. This spacer, 7–11 nm thick, was e-gun deposited on both the screened and reference samples simultaneously using pure quartz as the source. The Anderson insulator that was chosen for these experiments was the version of In_xO with a low carrier concentration ($N \leqslant 2 \times 10^{19}\,\mathrm{cm}^{-3}$). This version has several attractive features for these experiments: In the first place, the relatively large intercarrier distance $N^{-1/3} \simeq 5$ nm allows the spacer d to be thick enough to minimize pinholes while $dN^{1/3}$ may still be small enough for effective screening. Second, the electron-glass dynamics becomes faster as the carrier concentration falls below $N \lesssim 4 \times 10^{19}\,\mathrm{cm}^{-3}$, while, all other things being equal, the relative value of the excess conductance in the excited state $\Delta G/G$ is more conspicuous than in samples with $N > 4 \times 10^{19}\mathrm{cm}^{-3}$. These expectations were borne out in our experiments, which made it possible to quantify the system dynamics as it approaches the quantum phase transition.

Conductivity of the samples was measured using a two-terminal ac technique employing a 1211-ITHACO current preamplifier and a PAR-124A lock-in amplifier. Measurements were performed with the samples immersed in liquid helium at $T \approx 4.1$ K held by a 100-L storage dewar. This allowed up to 2 months of measurements on a given sample while keeping it cold. These conditions are essential for the measurements described below, where extended times of relaxation processes are required at a constant temperature, especially when running multiple excitation-relaxation experiments on the same sample.

The gate-sample voltage (referred to as V_g in this work) in the field-effect measurements was controlled by the potential difference across a 10-μF capacitor charged with a constant current fed by the Keithley K220. The rate of change of V_g is determined by the value of this current. The range of V_g used in this study reached, in some cases, ±50 V, which is equivalent to the ±12 V used in previous studies where the gate-sample separation was 0.5 μm compared with the 2-μmSiO_2 spacer used here.

The ac voltage bias in conductivity measurements was small enough to ensure near-Ohmic conditions. The voltage used in the relaxation experiments was checked to be in the linear response regime by plotting the current-voltage characteristics of each sample.

III. RESULTS AND DISCUSSION

A. Modifying the memory dip with a screening plane

The idea behind the use of the elaborate construction described in Fig. 1 was to find the effect of eliminating (or at least weakening) the long-range part of the Coulomb interaction. This relies on comparing results of identical measurements on the screened and reference samples. For that to be a tenable procedure, one has to ascertain that the two samples differ *only* by the image charges created in the nearby gold layer. This is not a trivial undertaking as the act of depositing the gold layer may inadvertently break the symmetry between the reference and screened samples. For example, the heat produced during deposition of the gold layer will unavoidably cause some annealing in the screened sample. A different disorder in the screened sample may also arise from the strain related to mismatch in the mechanical properties of the Au/SiO_2 interface. In principle, a difference in disorder between the screened and reference samples can be compensated by a judicious thermal annealing of the samples to make their room-temperature resistivities close to one another. However, being Anderson insulators, a few percent difference in room-temperature resistance may translate to orders of magnitude disparity at liquid-helium temperatures.

Fortunately, the feature that is targeted for investigation here is not susceptible to these artifacts. The *shape* of the memory dip (MD) which reflects the underlying Coulomb gap is a robust feature. At a given temperature, the MD shape is *independent* of the sample disorder, the sweep rate, time since cooldown, magnetic fields, etc.; it depends *only* on the carrier concentration, which is set by the In/O ratio, as

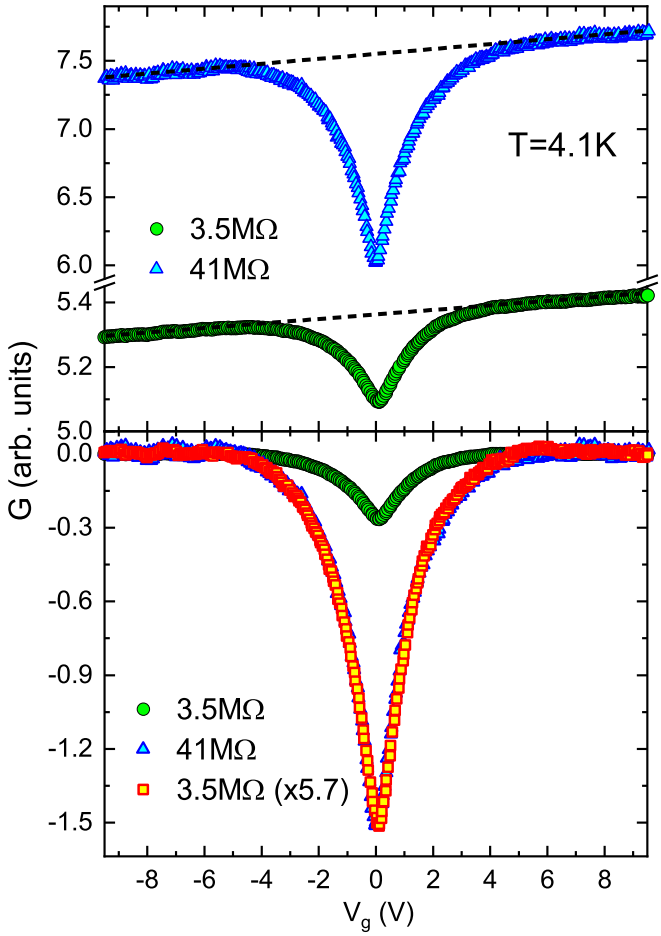

FIG. 2. The top panel shows field-effect plots $G(V_g)$ for two In_xO samples prepared from the same evaporation batch ($N = 8.7 \times 10^{19}\,cm^{-3}$) but subjected to different thermal annealing. The dashed lines depict the thermodynamic component of the respective $G(V_g)$. The bottom panel shows the MDs of these samples (after subtracting their respective thermodynamic component) and demonstrates that their magnitude may be made to scale just by a multiplicative constant.

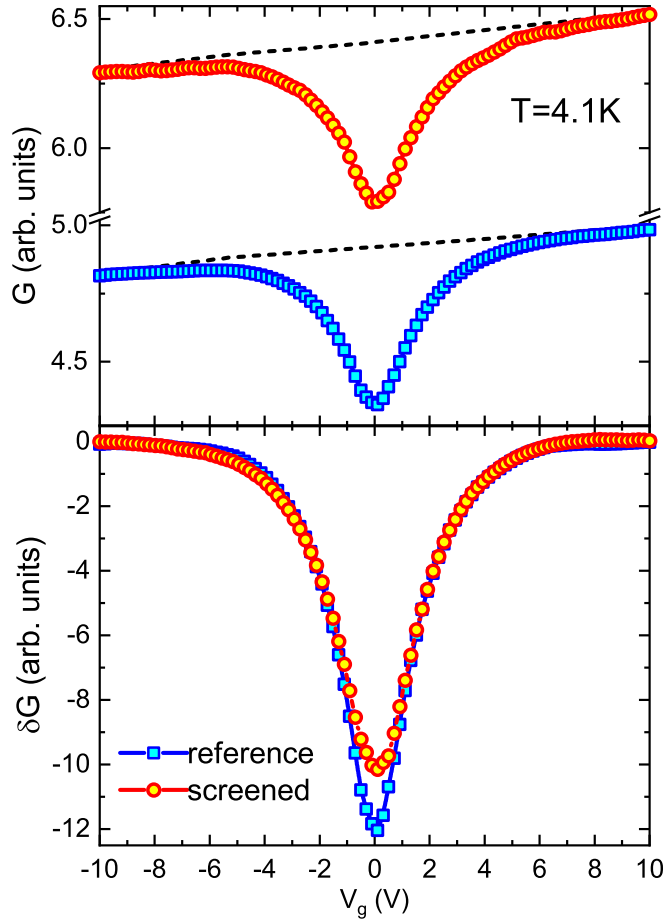

FIG. 3. Field-effect plots comparing $G(V_g)$ for a reference (squares) vs screened (circles) In_xO samples from the same evaporation batch as in Fig. 2. The bottom panel is an attempt to scale the MDs by a constant factor showing a reasonable fit for the wings, but the screened MD falls short of the reference MD for the bottom part of $G(V_g)$.

demonstrated in [7]. To illustrate, Fig. 2 shows the dependence of the conductance G on gate voltage V_g for two of the studied reference samples. These share the same composition but were subjected to different degrees of annealing and thus exhibit different sheet resistances (and thus disorder).

The top panel of Fig. 2 shows the raw data for the field effect $G(V_g)$ of these samples. Two features are observed: an asymmetric component characterized by $\partial G(V_g)/\partial V_g > 0$ that reflects the increased thermodynamic density of states with energy (the thermodynamic field effect) and a cusplike dip centered at $V_g = 0$, where the system was allowed to relax before sweeping the gate voltage (the memory dip). By subtracting from each plot the respective thermodynamic $G(V_g)$ component, one gets the two MDs that, after multiplication by a constant, are shown to have the same shape despite the large disparity in their resistance.

By contrast, the MDs of the reference-screened samples fail to show a similar data collapse. Figure 3 shows the results of an attempt to match the memory dips for a specific couple. In this case, the factor scaling the data for the two memory dips is possible for most of the range of $G(V_g)$ but not near its equilibrium point, where the screened dip falls short of the reference. Figure 4 shows, however, that the current-field characteristics of these samples are nearly identical even deeper into the non-Ohmic regime, and there is no sign of a current short from the active sample to the screening layer.

Note that in this pair, the resistance of the screened sample was larger than that of the reference. The cutback-shaped MD of the screened sample relative to the reference was observed in all six pairs studied in this work. The scaled results for a pair where the sheet resistance $R_\square$ of the screened sample is smaller than that of the reference sample are shown in Fig. 5, which depicts the same qualitative features as in Fig. 3. Finally, Fig. 6 shows two more reference-screened pairs taken from a single specific deposition batch with carrier concentration $N \approx 1.9 \times 10^{19}\,cm^{-3}$. Figure 6 includes both $R_\square$ (reference) $> R_\square$ (screened) and $R_\square$ (reference) $< R_\square$ (screened) cases as well as an extended range of the field effect vs a higher-resolution view of the memory-dip main features. Screening by a nearby metallic plane has been

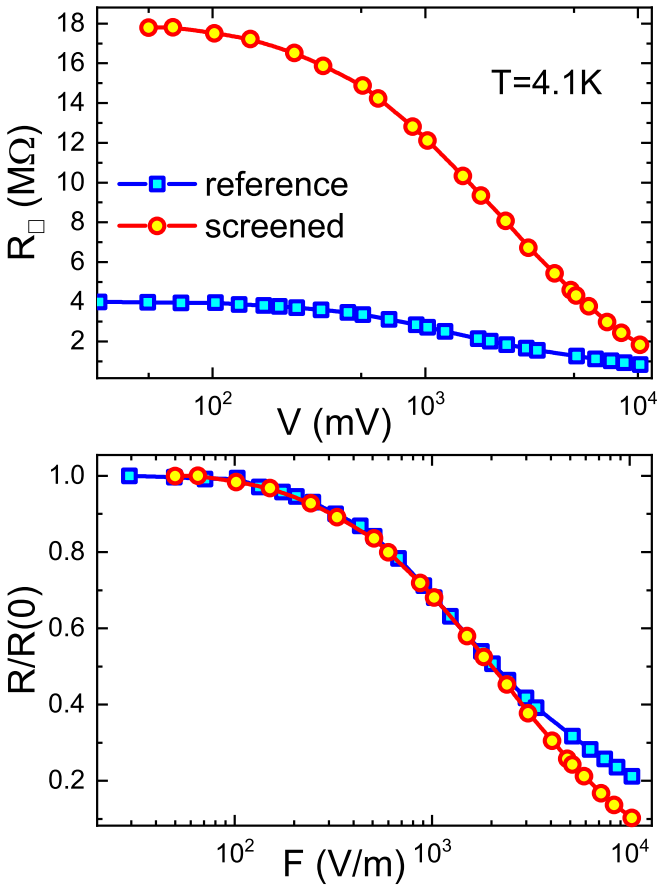

FIG. 4. Top: The dependence of the sheet resistance $R_\square$ of the screened (circles) and reference (squares) samples on the applied voltage (same samples as in Fig. 3). Bottom: The relative change of these resistances, showing a similar functional dependence.

shown to change the spatial dependence of the Coulomb interaction even in diffusive systems. Some features of the single-particle DOS found in tunneling experiments on two- and three-dimensional indium oxide samples differed in both

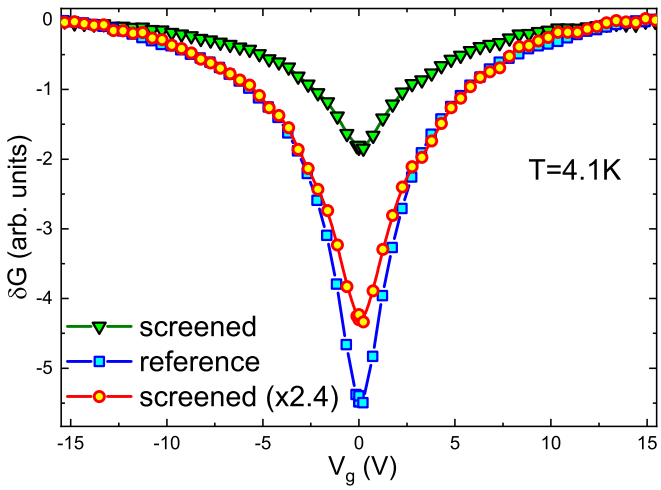

FIG. 5. Comparing the MD shape of a reference sample with $R_\square = 6.3$ MΩ with a screened sample of the same deposition batch with $R_\square = 3.1$ MΩ.

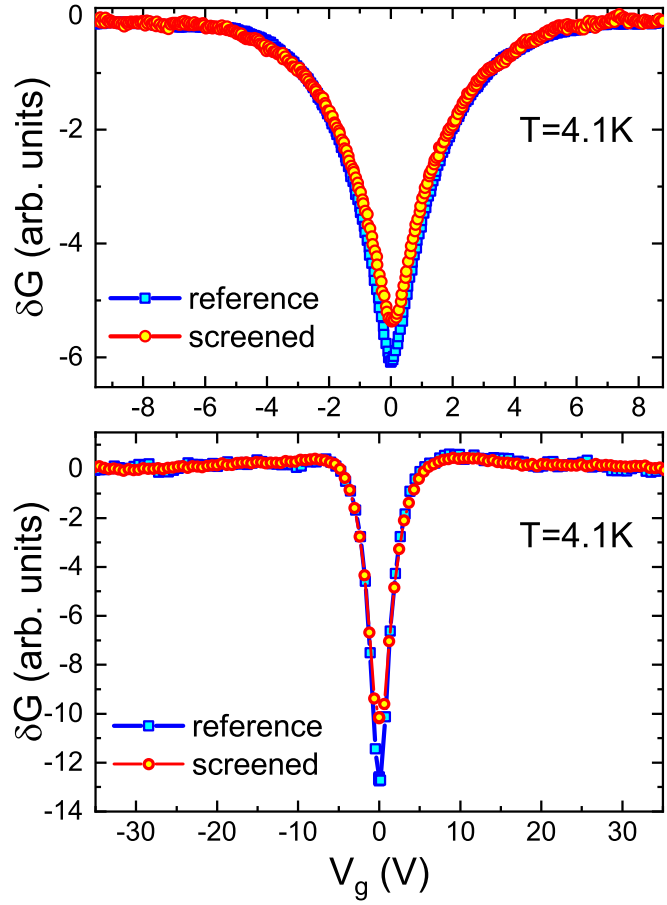

FIG. 6. Attempting to scale the functional dependence of the MD of a reference-screened pair of samples from the same deposition batch (with $N \approx 1.9 \times 10^{19}\,\mathrm{cm}^{-3}$). Top: Reference sample with $R_\square = 4$ MΩ and screened sample with $R_\square = 40$ MΩ. Bottom: Reference sample with $R_\square = 6.7$ MΩ and screened sample with $R_\square = 45$ MΩ.

magnitude and functional dependence from those predicted by simple models of interaction and disorder [20]. These differences were accounted for by Altshuler *et al.* based on the image charges created due to the proximity of the sample to the tunneling electrode [21]. The lack of screening in the Anderson-insulating phase makes the system more susceptible to the influence of the nearby metallic plane. A modified form of the Coulomb interaction is therefore an expected effect [22]. Indeed, the reduced relative magnitude of the screened MD observed in the current experiments is consistent with the effect of a screening layer on the Coulomb gap of a two-dimensional system. This effect was estimated theoretically by Hadley *et al.* [18]. In our six samples the reduced magnitude of the MD of the screened sample ranged between ≈12% and ≈23%, which, according to [18], is associated with $dN^{1/3} \approx 2.8$ to ≈1.6, respectively. For the carrier concentrations used in this work, $N = 8.7 \times 10^{19}$ to $1.9 \times 10^{19}\,\mathrm{cm}^{-3}$, these values give d in the range 8–15 nm, which is in good agreement with the thickness of the SiO_2 spacer used (see Sec. II). In the six pairs of screened and reference samples, however, it was not possible to see a systematic dependence on the spacer d. This is probably due to relatively large thickness variations in these thin films; both SiO_2 and In_xO have been

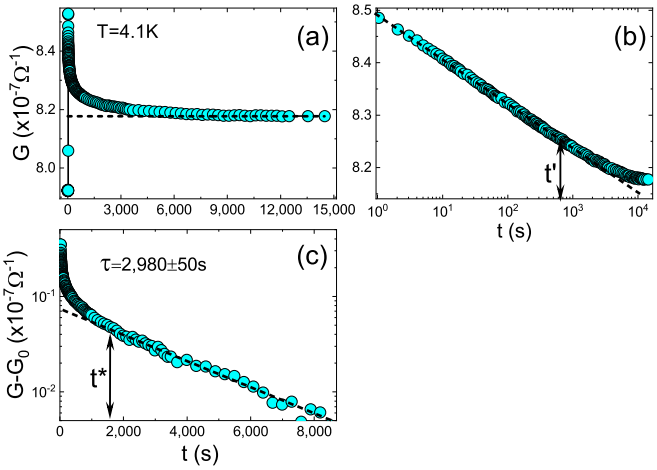

FIG. 7. Results of using the gate protocol (see text) on a sample with $R_\square = 1.2$ MΩ. (a) Conductance as a function of time; after ≈30 s of monitoring G under $V_g = 0$ V the gate voltage was swept to $V_g = 40$ V at a rate of 15 V/s. The dashed line is G_0, the asymptotic value of the conductance. $G_0 = G(40\,\mathrm{V})$ differs from $G(\mathrm{V_{eq}})$ due to the component of the thermodynamic field effect. (b) Conductance relaxation starting from the time $V_g = 40$ V was established, showing the extent of the logarithmic dependence (delineated by the dashed line). t' marks the point where $G(t)$ deviates from the logarithmic dependence. (c) The plot of $G(\mathrm{t})-G_0$ demonstrating an exponential relaxation law: $\Delta G(t) \propto \exp[-(t/\tau)]$ (the dashed line is the best fit, yielding the relaxation time τ for the sample). t^* marks the time below which $G(t)$ deviates from exponential relaxation.

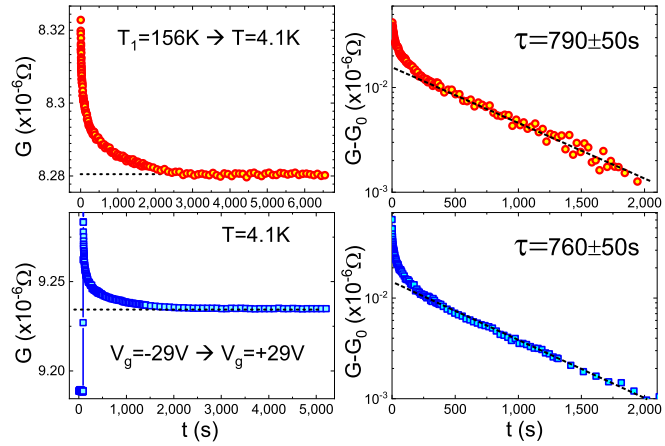

FIG. 8. The relaxation dynamics of an $\mathrm{In}_x\mathrm{O}$ film with $R_\square = 0.13$ MΩ at 4.1 K and $N \approx 1.9 \times 10^{19}\,\mathrm{cm}^{-3}$ tested by two protocols. Top: Using a quench-cool protocol. Bottom: Using the gate protocol. Dashed lines delineate the equilibrium conductance G_0 for each protocol. The relaxation time τ is obtained from the fit to $\Delta G(t) \propto \exp[-(t/\tau)]$ for the data in the two right plots.

tested by atomic-force microscopy, which showed thickness fluctuations of the order of ±8% [23].

It is natural to ask how limiting the interaction range affects how the system thermalizes after being taken out of equilibrium; attempts to answer this question are discussed next.

B. Thermalization dynamics

1. Experimental definition of the thermalization time

It is rarely possible to ascertain experimentally that a system under observation is thermalized. One may, however, monitor the process of the approach towards equilibrium by following a specific measurable quantity and associate the state of thermalization with the time where this measured quantity reaches a time-independent value relative to which the system just fluctuates. Thermalization and relaxation will be used here interchangeably, although, technically, the time-independent regime may only signal prethermalization.

An effective way to take the system far from equilibrium and observe the ensuing relaxation is the "gate protocol." In this protocol a nonequilibrium state is created by switching the gate voltage V_g from an equilibrium value V_{eq} to a new one, V_n. This process is reflected in the appearance of excess conductance $\Delta G(t)$ that decays slowly with time. An example of the results obtained with this protocol is shown in Fig. 7.

The relaxation to the equilibrium under the newly established V_n was monitored through the measured $\Delta G(t)$. As observed in Fig. 7, $\Delta G(t) \propto -\ln(t)$ for several hundred seconds [up to t' in Fig. 7(b)], and after a time marked t^* [Fig. 7(c)] the relaxation law reverts to $\Delta G(t) \propto \exp[-t/\tau]$, which defines τ, which will be used here as the characteristic thermalization time. As will be shown in the next paragraph, when properly implemented, this gate protocol is equivalent to quench cooling the system from high temperatures. The latter has the advantages of being history free, but the thermal cycle runs the risk of changing the structure of the sample (and possibly damage it more seriously), and it also sacrifices the short-time relaxation because one must wait for the sample and its surroundings (sample stage, thermometer, etc.) to cool to the bath temperature. The gate protocol, by contrast, may be safely repeated many times on the same sample, and no "parasitic" heating is involved in the process.

An important caveat when using the gate protocol is to let the sample reach equilibrium before changing the gate voltage to a new value to avoid history dependence [24]. As a check on this point, we compared the relaxation time of a sample using both a thermal quench and the gate protocol. The results, shown in Fig. 8, demonstrate that the relaxation time τ based on the gate protocol is essentially identical to that based on quench cooling the sample. We believe that the gate protocol can be relied upon to yield the correct relaxation time, provided the equilibration time is longer than τ. For the series of measurements reported below, the samples were equilibrated under V_{eq} for at least 12 h under V_{eq}.

2. Dynamics of screened and reference samples

Comparing screened and reference samples is more problematic when it comes to dynamics than the difficulties mentioned above with regard to the effect on the shape of the memory dip. The latter is independent of the disorder; the MD shape is the same even when the sample $R_\square$ changes by an order of magnitude (see Fig. 2), while the dynamics is quite sensitive to the sample disorder [17], as will be demonstrated below. Figure 9 shows $\Delta G(t)$ for the asymptotic relaxation regime generated by using the gate protocol. These

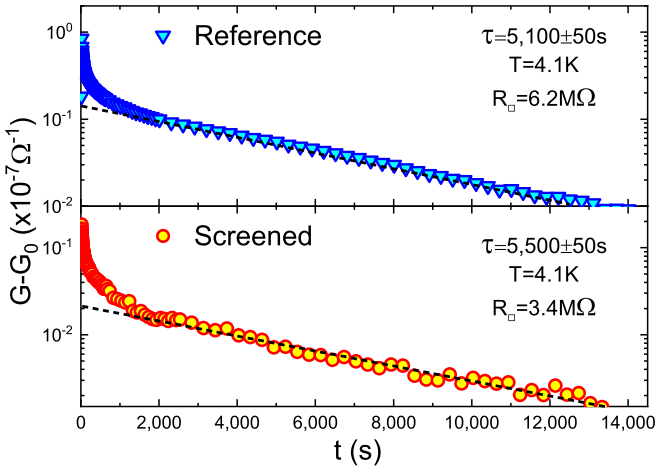

FIG. 9. The asymptotic relaxation curves for a specific In_xO screened-reference pair ($N \approx 1.9 \times 10^{19}$ cm^{-3}) using the gate protocol under identical conditions. Dashed lines are best fits to $\Delta G(t) \propto \exp[-(t/\tau)]$ that yielded the respective relaxation time shown in the panels.

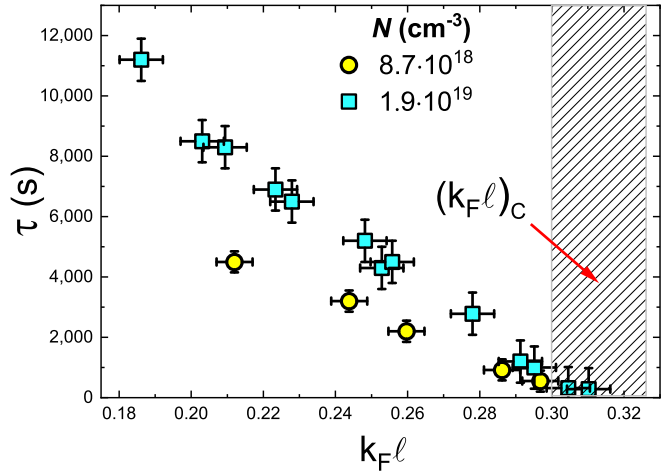

FIG. 10. The dependence of the relaxation times τ (as defined in Figs. 7 and 8) on the disorder parameter $k_F\ell$ near the critical regime of the metal-to-insulator transition (marked by the hatched area).

data were taken on the same samples used for comparing the MD shapes in Fig. 5 that, in terms of their $R_\square$, are our best-matched screened-reference pair. The data in Fig. 9 clearly suggest that the relaxation time of the screened sample is essentially the same as the reference. Therefore, limiting the range of the Coulomb interaction to ≈8 nm does not have a significant effect on the system relaxation time. Moreover, τ of the order of a few thousand seconds is manifestly possible even *without long-range interaction*. This is a useful piece of information that should make it easier for theory to finally address the long-standing question of the slow relaxation times of some electron glasses [24]. We return to this issue after discussing the results of the dynamics as a function of disorder.

3. Disorder vs interaction

To get a better picture of the dynamics we expanded a preliminary study of In_xO films with low carrier concentration $N = 8.7 \times 10^{19}$ cm^{-3} [25] by measuring 13 samples from the batch with $N = 1.9 \times 10^{19}$ cm^{-3}, with which most of the screened and reference samples studied here were made.

Figure 10 shows the relaxation time τ (defined by the exponential-relaxation regime of the gate protocol) as a function of the dimensionless parameter $k_F\ell$. As in other studies [26,27], $k_F\ell = (3\pi^2)^{2/3}\hbar\sigma_{RT}e^{-2}N^{-1/3}$ was taken as the measure of the quenched disorder (σ_{RT} is the sample conductivity at room temperature).

There are two interesting features that emerge from the data. First, the relaxation time decreases with $k_F\ell$ and tends to zero roughly at the disorder range where the system undergoes the metal-to-insulator transition. The critical value of disorder $(k_F\ell)_C$ for the metal-insulator transition was independently measured for two versions of the material with $N \approx 10^{21}$ cm^{-3} [26] and $N \approx 10^{19}$ cm^{-3} [27], yielding in both $(k_F\ell)_C = 0.31 \pm 0.03$. That the glassy features end at the transition is an important finding; it supports the conjecture that the slow relaxation is an electronic effect rather than reflecting structural defects. Note that the reduction of τ with $k_F\ell$ is achieved in In_xO by thermal annealing. Changes in the structural properties of the material during the annealing process were extensively studied in [17] by electron diffraction, energy-dispersive spectroscopy, x-ray interferometry, and optical techniques. The study revealed that the change in the resistance from the as-deposited deeply insulating state all the way to the metallic regime is mainly due to an increase of the material *density*. In particular, the samples retained their amorphous structure and composition throughout the entire process. Moreover, the dynamics associated with structural changes monitored during annealing and recovery of the samples was qualitatively different from that of the electron glass and did not change its character throughout the entire range of disorder. The diminishment of τ with $k_F\ell$ cannot then be identified with the elimination of some peculiar structural defects. Second, the relaxation time is not a function of just $k_F\ell$; it appears that it also depends on the carrier concentration N. Indeed, the exponential relaxation regime (which allows an unambiguous definition of τ) become quickly out of reach for samples when $N \geqslant 5 \times 10^{19}$ cm^{-3}. The data in Fig. 10 seem to suggest a scaling relation of the form

$$\tau = \tau(N)[k_F\ell - (k_F\ell)_C], \quad k_F\ell \geqslant (k_F\ell)_C,$$

where the prefactor $\tau(N)$ presumably increases with carrier concentration. One may surmise that the dependence on N may be the effect of interactions. The logic is based on the realization that, due to the lack of electronic screening of the Anderson insulator, the higher density of carriers enhances the strength of the interaction. While it is plausible that interactions in the localized system get stronger with N, it is not necessarily the main (or the only) reason for slower relaxation [17]. It is here that the issue of separating the effects of Coulomb interaction from the effect of disorder presents

a frustrating problem because interaction and disorder both increase with N. Actually, a viable cause for τ increasing with N is the higher degree of disorder in samples that have higher carrier concentrations. Note that a precondition for the electronic system to exhibit slow relaxation is Anderson localization [17]. This requires that the disorder energy $\mathcal{W}$ has to be larger than the Fermi energy E_F by a certain factor [28,29]. All other things being equal, a system with a larger carrier concentration N must be more disordered to be Anderson localized and thus has larger $\mathcal{W}$. This, in turn, will *exponentially* slow down the intersite transitions, whether activated or through tunneling.

The way that Coulomb interactions affect thermalization dynamics is less clear. Interactions may modify transition rates through the reduction of the density of states, and many-particle transitions may be involved in the process, but it is hard to find experimental evidence that may be uniquely related to these mechanisms. A large magnitude of memory dip, suggestive of a more dominant role of interactions, is actually found in low-N systems where the dynamics is relatively fast, as found in the present study. This, however, does not mean that interactions act to speed up thermalization; rather, it shows that the disorder effect (being weaker at low N) is more important. A possible example for enhanced carrier concentration without the accompanying increase of disorder was observed in GeSbTe samples in their persistent photoconductive state [30]. This caused an enhanced magnitude of the memory dip, which was interpreted as an interaction effect [30]. It also slowed down the dynamics, but interaction is not the only possible mechanism for it; the slow decay of the photoinduced carriers may be the more mundane reason.

The transition to the exponential relaxation at long times, as observed, for example, in Fig. 7, is expected. A $\ln(t)$ relaxation is limited to intermediate times; it has to cross over to a different form for both short and long times [31]. The transition from the logarithmic to the exponential-relaxation regime is preceded by a more complicated time dependence which perhaps resembles the fast relaxation observed in phosphorous-doped silicon [32]. This region extends over a time period that grows monotonically with disorder [33], as is shown in Fig. 11.

The dependence of the dynamics on $k_F\ell$ may be summarized as follows: As $k_F\ell$ increases and the system approaches the diffusive regime, the rate distribution, which controls the relaxation from an excited state, gets narrower due to the reduction of the lowest transition rates (associated with the τ deduced from the exponential-relaxation regime). Concomitantly, the range over which logarithmic relaxation is observed shrinks linearly with $k_F\ell$ (Fig. 11).

It is intriguing that the time period for the logarithmic relaxation in an electron glass may extend over almost six decades [24] without a sign of a crossover. To account for such an extensive range one has to assume a fairly uniform distribution of transition rates over a wide frequency range. It seems obvious that a main ingredient in the underlying mechanism

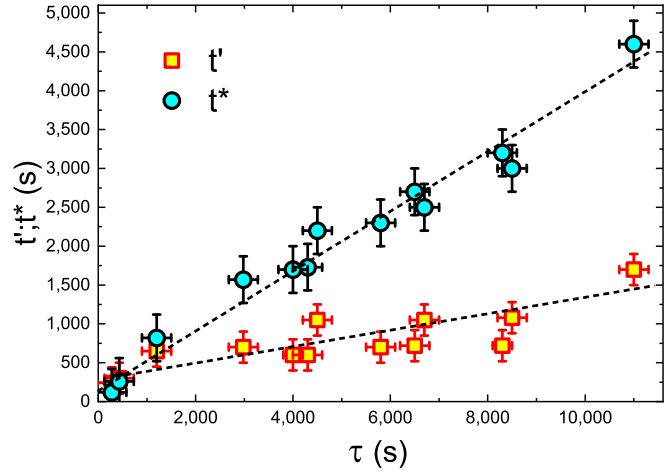

FIG. 11. The end times for the logarithmic and simple exponential relaxations, t' and t^*, respectively, as a function of τ for the samples studied by the gate protocol in Fig. 10.

is sufficiently strong disorder, but it probably also involves many-body effects [34]. The current study demonstrated that electronic relaxation extending over thousands of seconds is a viable possibility without the long-range part of the Coulomb interaction playing a significant part (and therefore, the DOS at the Fermi energy must be finite even at $T = 0$).

It is harder to assess the contribution of short- and medium-range Coulomb interaction to the dynamics. One might argue that the faster dynamics observed as the system approaches the metallic regime may, at least in part, be due to the enhanced dielectric constant that, in turn, weakens the interaction. The dielectric constant in the localized state is expected to increase significantly near the transition [35]. However, the functional dependence of $\tau(k_F\ell)$ shown in Fig. 10 does not exhibit a change from the linear dependence as the transition is approached. Therefore, this scenario is not supported by our experiments. Interactions are more likely to play a significant role in the ultraslow processes that are necessary to reach the true ground state of the system, a process that presumably hinges on many-particle transitions [36].

There are other mechanisms that may contribute to stretching the transition-rate distribution and afford an extended logarithmic dependence. Reduction of transition rates relative to the "bare" rates controlled by disorder may occur for nonlocal interactions. These may bring into play additional constraints as well as effects related to coupling of the tunneling charge to other degrees of freedom (polaronic effects and the orthogonality catastrophe [37–39]). Resolution of these issues remains a challenge to theory.

ACKNOWLEDGMENTS

Illuminating discussions with A. Vaknin and M. Schechter are gratefully acknowledged. This research has been supported by Grant No. 1030/16 administered by the Israel Academy for Sciences and Humanities.

[1] P. W. Anderson, Phys. Rev. **109**, 1492 (1958).

[2] L. Fleishman and P. W. Anderson, Phys. Rev. B **21**, 2366 (1980).

[3] I. V. Gornyi, A. D. Mirlin, and D. G. Polyakov, Phys. Rev. Lett. **95**, 206603 (2005).

[4] D. M. Basko, I. L. Aleiner, and B. L. Altshuler, Ann. Phys. (NY) **321**, 1126 (2006).

[5] V. Oganesyan and D. A. Huse, Phys. Rev. B **75**, 155111 (2007); R. Nandkishore and D. A. Huse, Annu. Rev. Condens. Matter Phys. **6**, 15 (2015).

[6] M. Ben-Chorin, D. Kowal, and Z. Ovadyahu, Phys. Rev. B **44**, 3420 (1991); M. Ben-Chorin, Z. Ovadyahu, and M. Pollak, *ibid.* **48**, 15025 (1993).

[7] A. Vaknin, Z. Ovadyahu, and M. Pollak, Phys. Rev. B **65**, 134208 (2002).

[8] J. H. Davies, P. A. Lee, and T. M. Rice, Phys. Rev. Lett. **49**, 758 (1982); M. Grünewald, B. Pohlman, L. Schweitzer, and D. Würtz, J. Phys. C **15**, L1153 (1982); J. H. Davies, P. A. Lee, and T. M. Rice, Phys. Rev. B **29**, 4260 (1984); C. C. Yu, Phys. Rev. Lett. **82**, 4074 (1999).

[9] M. Müller and L. B. Ioffe, Phys. Rev. Lett. **93**, 256403 (2004).

[10] V. Malik and D. Kumar, Phys. Rev. B **69**, 153103 (2004).

[11] R. Grempel, Europhys. Lett. **66**, 854 (2004); A. B. Kolton, D. R. Grempel, and D. Dominguez, Phys. Rev. B **71**, 024206 (2005).

[12] E. Lebanon and M. Müller, Phys. Rev. B **72**, 174202 (2005); M. Müller and E. Lebanon, J. Phys. IV **131**, 167 (2005).

[13] A. Amir, Y. Oreg, and Y. Imry, Phys. Rev. B **77**, 165207 (2008); Annu. Rev. Condens. Matter Phys. **2**, 235 (2011).

[14] Y. Meroz, Y. Oreg, and Y. Imry, Europhys. Lett. **105**, 37010 (2014).

[15] M. Pollak, M. Ortuño, and A. Frydman, *The Electron Glass* (Cambridge University Press, Cambridge, 2013).

[16] M. Pollak, Discuss. Faraday Soc. **50**, 13 (1970); A. L. Efros and B. I. Shklovskii, J. Phys. C **8**, L49 (1975).

[17] Z. Ovadyahu, Phys. Rev. B **95**, 134203 (2017).

[18] B. Hadley, M. Green, M. Pollak, R. Chicon, and M. Ortuño, J. Non-Cryst. Solids **97–98**, 233 (1987).

[19] Z. Ovadyahu, Phys. Rev. B **95**, 214207 (2017).

[20] Y. Imry and Z. Ovadyahu, Phys. Rev. Lett. **49**, 841 (1982).

[21] B. L. Altshuler, A. G. Aronov, and A. Yu. Zyuzin, Zh. Eksp. Teor. Fiz. **86**, 709 (1984) [Sov. Phys. JETP **59**, 415 (1984)].

[22] A. I. Larkin and D. E. Khmel'nitskii, Zh. Eksp. Teor. Fiz. **83**, 1140 (1982) [Sov. Phys. JETP **56**, 647 (1982)].

[23] A. Frydman and Z. Ovadyahu, Phys. Rev. B **55**, 9047 (1997).

[24] Z. Ovadyahu and M. Pollak, Phys. Rev. B **68**, 184204 (2003).

[25] Z. Ovadyahu, Phys. Rev. B **97**, 214201 (2018).

[26] D. Shahar and Z. Ovadyahu, Phys. Rev. B **46**, 10917 (1992).

[27] U. Givan and Z. Ovadyahu, Phys. Rev. B **86**, 165101 (2012).

[28] B. R. Bulka, B. Kramer, and A. MacKinnon, Z. Phys. B **60**, 13 (1985).

[29] B. Bulka, M. Schreiber, and B. Kramer, Z. Phys. B **66**, 21 (1987).

[30] Z. Ovadyahu, Phys. Rev. Lett. **115**, 046601 (2015); Phys. Rev. B **97**, 054202 (2018).

[31] G. Mihàly and L. Mihàly, Phys. Rev. Lett. **52**, 149 (1984).

[32] V. K. Thorsmølle and N. P. Armitage, Phys. Rev. Lett. **105**, 086601 (2010).

[33] This part of the relaxation may be fitted to a stretched-exponential function $\Delta G(t) = A\exp[-(t/\tau')^{\beta}]$ by adjusting the parameters $\tau'$and β. For example, the data for the intermediate range of $15\,\mathrm{s} \leqslant t \leqslant 5\times10^{3}\,\mathrm{s}$ in Fig. 7(c) may be fitted with the three parameters $A = 3.3\times10^{-8}\,\Omega^{-1}$, $\tau' = 185$ s, and $\beta = 0.33$.

[34] M. Pollak and M. Ortuño, Sol. Energy Mater. **8**, 81 (1982); M. Pollak, Philos. Mag. B **50**, 265 (1984).

[35] T. G. Castner, N. K. Lee, G. S. Cieloszyk, and G. L. Salinger, Phys. Rev. Lett. **34**, 1627 (1975); D. Stroud and D. J. Bergman, Phys. Rev. B **25**, 2061(R) (1982); H. S. Choi, J. S. Ahn, J. H. Jung, T. W. Noh, and D. H. Kim, *ibid.* **54**, 4621 (1996).

[36] S. D. Baranovskii, B. I. Shklovskii, and A. L. Efros, Zh. Eksp. Teor. Fiz. **51**, 199 (1980) [Sov. Phys. JETP **51**, 199 (1980)]; A. Möbius, M. Richter, and B. Drittler, Phys. Rev. B **45**, 11568 (1992); A. L. Efros, B. Skinner, and B. I. Shklovskii, *ibid.* **84**, 064204 (2011).

[37] P. W. Anderson, Phys. Rev. Lett. **18**, 1049 (1967); A. J. Leggett *et al.*, Rev. Mod. Phys. **59**, 1 (1987); Z. Ovadyahu, Phys. Rev. Lett. **99**, 226603 (2007).

[38] V. Khemani, R. Nandkishore, and S. L. Sondhi, Nat. Phys. **11**, 560 (2015).

[39] D.-L. Deng, J. H. Pixley, X. Li, and S. Das Sarma, Phys. Rev. B **92**, 220201(R) (2015).